

## Level, distribution and sources of Np, Pu and Am isotopes in Peter the Great Bay of Japan sea

Jiang Sun<sup>b</sup>, Shaodong Zhu<sup>b</sup>, Shan Xing<sup>a,b,\*</sup>, Natalia V. Kuzmenkova<sup>c</sup>, Chenyang Peng<sup>b</sup>, Yiman Lu<sup>b</sup>, Alexandra Rozhkova<sup>c</sup>, Vladimir G. Petrov<sup>c</sup>, Keliang Shi<sup>a,b</sup>, Stepan N. Kalmykov<sup>c</sup>, Xiaolin Hou<sup>a,b,\*\*</sup>

<sup>a</sup> Frontiers Science Center for Rare Isotopes, Lanzhou University, Lanzhou 73000, China

<sup>b</sup> School of Nuclear Science and Technology, Lanzhou University, Lanzhou 730000, China

<sup>c</sup> Department of Chemistry, Division of Radiochemistry, Lomonosov Moscow State University, Moscow 119991, Russia

### ARTICLE INFO

#### Keywords:

Transuranium radionuclides  
Japan sea  
Sources  
Environmental radioactivity  
Migration behaviors

### ABSTRACT

Transuranium elements such as Np, Pu and Am, are considered to be the most important radioactive elements in view of their biological toxicity and environmental impact. Concentrations of <sup>237</sup>Np, Pu isotopes and <sup>241</sup>Am in two sediment cores collected from Peter the Great Bay of Japan Sea were determined using radiochemical separation combined with inductively coupled plasma mass spectrometry (ICP-MS) measurement. The <sup>239,240</sup>Pu and <sup>241</sup>Am concentrations in all sediment samples range from 0.01 Bq/kg to 2.02 Bq/kg and from 0.01 Bq/kg to 1.11 Bq/kg, respectively, which are comparable to reported values in the investigated area. The average atomic ratios of <sup>240</sup>Pu/<sup>239</sup>Pu ( $0.20 \pm 0.02$  and  $0.21 \pm 0.01$ ) and <sup>241</sup>Am/<sup>239+240</sup>Pu activity ratios ( $3.32 \pm 2.76$  and  $0.45 \pm 0.17$ ) in the two sediment cores indicated that the sources of Pu and Am in this area are global fallout and the Pacific Proving Grounds through the movement of prevailing ocean currents, and no measurable release of Np, Pu and Am from the local K-431 nuclear submarine incident was observed. The extremely low <sup>237</sup>Np/<sup>239</sup>Pu atomic ratios ( $(2.0\text{--}2.5) \times 10^{-4}$ ) in this area are mainly attributed to the discrepancy of their different chemical behaviors in the ocean due to the relatively higher solubility of <sup>237</sup>Np compared to particle active plutonium isotopes. It was estimated using two end members model that 23%  $\pm$  6% of transuranium radionuclides originated from the Pacific Proving Grounds tests, and the rest (ca. 77%) from global fallout.

### 1. Introduction

Isotopes of transuranium elements such as neptunium (Np), plutonium (Pu) and americium (Am) have long half-lives (<sup>237</sup>Np,  $T_{1/2} = 2.14 \times 10^6$  y; <sup>239</sup>Pu,  $T_{1/2} = 2.44 \times 10^4$  y; <sup>240</sup>Pu,  $T_{1/2} = 6.58 \times 10^3$  y; <sup>241</sup>Am,  $T_{1/2} = 432.7$  y) and high biological toxicity (Dozol et al., 1993; Beasley et al., 1998; Assinder, 1999). In general, these isotopes are mainly released into the environment as a result of major nuclear activities including atmospheric nuclear weapons testing, nuclear accidents (e.g., Chernobyl accident in 1986, Fukushima accident in 2011) as well as discharges from nuclear reprocessing facilities (e.g., La Hague, Sellafield) (Aarkrog, 2003; Zheng et al., 2012). The influences of transuranium radionuclides released from these major nuclear activities on the marine, atmospheric and terrestrial environment have been well

studied (Yoshida and Kanda, 2012; Buesseler et al., 2017). However, some small nuclear accidents (e.g., Russian K-431 submarine accident at Chazhma Bay in Japan Sea) were usually prone to be ignored (Sarkisov and Vysotskii, 2021). Therefore, the need for reasonable assessment of transuranium radionuclides released from the accident into the environment (e.g., marine) is even more pronounced.

Based on the ratios of <sup>240</sup>Pu/<sup>239</sup>Pu, <sup>237</sup>Np/<sup>239</sup>Pu and <sup>241</sup>Am/<sup>239+240</sup>Pu for specific sources, transuranium radionuclides in the environment have been used for source identification and contamination assessment (Hou and Roos, 2008; Huang et al., 2023a, 2023b; Ni et al., 2020). In general, the <sup>240</sup>Pu/<sup>239</sup>Pu atomic ratio is less than 0.07 for weapons-grade plutonium, 0.17–0.19 for global atmospheric deposition and 0.2–0.8 for nuclear fuel reprocessing (Kelley et al., 1999; Dai et al., 2002). The <sup>241</sup>Am/<sup>239+240</sup>Pu activity ratio can also provide useful

\* Corresponding author. at: Frontiers Science Center for Rare Isotopes, Lanzhou University, Lanzhou 73000, China.

\*\* Corresponding author. . Frontiers Science Center for Rare Isotopes, Lanzhou University, Lanzhou 73000, China.

E-mail addresses: [xings@lzu.edu.cn](mailto:xings@lzu.edu.cn) (S. Xing), [houlx@lzu.edu.cn](mailto:houlx@lzu.edu.cn) (X. Hou).

<https://doi.org/10.1016/j.jenvrad.2024.107400>

Received 17 November 2023; Received in revised form 8 February 2024; Accepted 10 February 2024

Available online 22 February 2024

0265-931X/© 2024 Elsevier Ltd. All rights reserved.

information for source identification. The  $^{241}\text{Am}/^{239+240}\text{Pu}$  activity ratio of 0.35 (decay corrected to 2022) in environmental samples only affected by the global atmospheric deposition was reported observed (Zheng et al., 2012). Although  $^{237}\text{Np}/^{239}\text{Pu}$  atomic ratio can also be used as a specific indicator to investigate the source of transuranium radionuclides in the environment, it often needs to be used in combination with other indicators since Np more easily migrates in the environment compared with Pu (Zhang et al., 2022). In addition, transuranium radionuclides from global and/or local releases into the environment can be considered as excellent tracers for the investigation of water circulation in the ocean (Dai et al., 2002; Wu et al., 2014).

The Japan Sea is the marginal sea in the northwestern Pacific Ocean and is connected with the East China Sea through the Tsushima Straits, the northwestern Pacific Ocean through the Tsugaru Strait, the Okhotsk Sea through Soya strait and Mamiya strait. Some studies have reported that the water mass from the Pacific Proving Grounds (PPG) can be transported from the north equatorial area to Japan Sea by the Kuroshio invasion, which can carry artificial long-lived radionuclides such as  $^{237}\text{Np}$  and  $^{239+240}\text{Pu}$  (Wang et al., 2022). Furthermore, the K-431 nuclear submarine accident in August 1985 caused a serious nuclear release at Peter the Great Bay of Japan Sea (Sarkisov and Vysotskii, 2021), used as a base of the Russian Pacific Fleet. Short half-life radionuclides (e.g.,  $^{60}\text{Co}$ ,  $^{90}\text{Sr}$ ,  $^{134}\text{Cs}$ ,  $^{137}\text{Cs}$ ,  $^{131}\text{I}$ ,  $^{133}\text{I}$ ) released from this accident have been measured in the marine environment and atmosphere near Vladivostok (Takano et al., 2001; Ikeuchi, 2003). To the best of our knowledge, no data have been reported so far for the level and distribution of Np, Pu and Am isotopes in this area.

This study aims to investigate the level, distribution and sources of transuranium radionuclides at Peter the Great Bay in Japan Sea, and to assess the impact of the K-431 nuclear submarine accident and other nuclear activities on the investigated area. This is achieved by analyzing sediment samples collected from this area for  $^{237}\text{Np}$ ,  $^{239}\text{Pu}$ ,  $^{240}\text{Pu}$  and  $^{241}\text{Am}$  using radiochemical separation and ICP-MS/MS measurement. The migration behaviors of  $^{237}\text{Np}$ ,  $^{239+240}\text{Pu}$  and  $^{241}\text{Am}$  in this area are also predicted.

## 2. Materials and methods

### 2.1. Sample collection

Peter the Great Bay is located in the northwestern part of the Japan Sea at the border of the temperate and subtropical zones (Fig. 1). Amur Bay and Ussuri Bay are the largest bays in Peter the Great Bay. The Razdolnaya river flows into the northern part of Amur Bay, which

extends from south-west to north-east for 70 km, with a width of 10–22 km and an average depth of 30 m. Many rivers, including Knevichanka River, Artemovka River, Shkotovka River as well as some other small rivers, flow into Ussuri Bay. Those rivers could carry a large amount of mud and sand into Ussuri Bay.

Two sediment cores of JS-2 with the length of 64 cm and JS-4 with the length of 34 cm were collected from Peter the Great Bay (43.15°N, 132°E) in 2022 (Fig. 1) using a modified percussion forcer tube with the diameter of 110 mm (Zheleznova et al., 2024). The sediment cores were stored in a 4 °C refrigerator and shipped to the laboratory within approximately two weeks. The sediment cores were sliced at 1 cm intervals and then the samples were freeze-dried in polyethylene containers. The dried samples were ground and sieved through a 200-mesh sieve. The samples were sealed in plastic bags and transported to the radiochemical laboratory in Lanzhou University, China for determination of transuranium radionuclides.

### 2.2. Sample preparation and measurement

The sediment samples were simultaneously analyzed for  $^{237}\text{Np}$ ,  $^{239}\text{Pu}$ ,  $^{240}\text{Pu}$  and  $^{241}\text{Am}$  using radiochemical separation in combination with ICP-MS/MS measurement. A brief description of the analytical method is presented here, and the detailed analytical method has been reported elsewhere (Xing et al., 2018, 2023). Briefly, about 2–5 g of the dried sample was ashed at 450 °C for at least 6 h. The ashed sample was spiked 0.5 pg of  $^{242}\text{Pu}$  and 0.5 pg of  $^{243}\text{Am}$  as yield tracers and then leached with 40 mL of aqua regia at 180 °C for 2.5 h on a hotplate. After cooling, the sample was filtered through a glass fiber filter of 2 μm in pore size, and ammonium and 50 mg of  $\text{TiOCl}_2$  were added to the leachate to co-precipitate Np, Pu and Am with HTiO by adjusting to pH 7–8. The precipitate was then dissolved in 8 mol/L  $\text{HNO}_3$  medium using concentrated  $\text{HNO}_3$ , and 0.02 mol/L  $\text{NaNO}_2$  was added to adjust the overall Np, Pu and Am to Np (VI), Pu (IV) and Am (III) in 8 mol/L  $\text{HNO}_3$  medium prior to chromatographic separation. Np, Pu and Am were separated and purified by using the TK200 resin and DGA resin columns (1 cm in diameter and 3.5 cm in length). Pu and Np were eluted from TK-200 resin with 40 mL of 0.5 mol/L HCl and 0.1 mol/L  $\text{NH}_2\text{OH}\cdot\text{HCl}$ , and Am was eluted from DGA resin with 40 mL of 0.05 mol/L HCl.

The separated Np, Pu and Am in eluates were heated to near dryness and dissolved in 3 mL 0.5 mol/L  $\text{HNO}_3$  for the measurement by ICP-MS/MS (Agilent 8900 ICP-MS, USA). The minimum detection limits of  $^{237}\text{Np}$ ,  $^{239}\text{Pu}$ ,  $^{240}\text{Pu}$  and  $^{241}\text{Am}$  were 1.8 fg, 6.7 fg, 3.0 fg, 0.9 fg, respectively. The results of measured certified reference materials are shown in Table S1. The accuracies of the  $^{237}\text{Np}$ ,  $^{239}\text{Pu}$ ,  $^{240}\text{Pu}$  and  $^{241}\text{Am}$

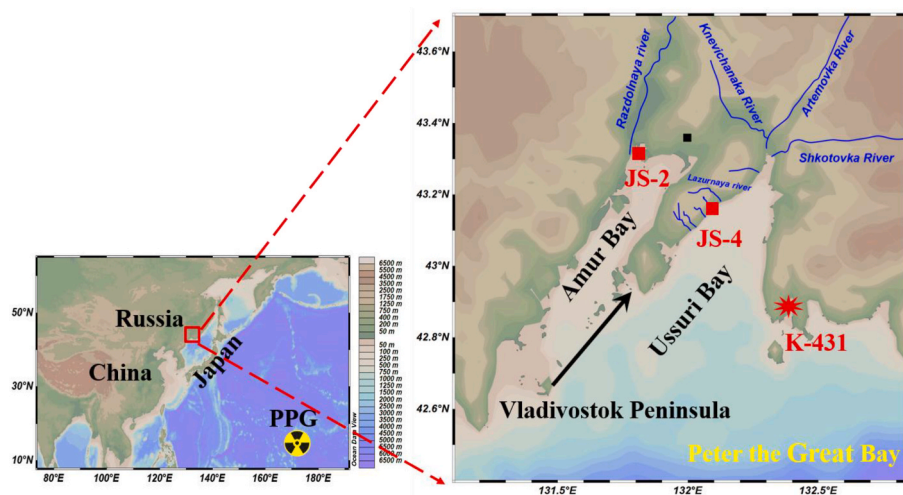


Fig. 1. Sampling sites of sediment cores in the northwest of Japan Sea (red squares) and K-431 nuclear leak accident. (For interpretation of the references to colour in this figure legend, the reader is referred to the Web version of this article.)

were in good agreement (within 95% confidence interval) with the certified and previously reported values. No significant discrepancies among the analytical results of  $^{237}\text{Np}$  ( $0.0019 \pm 0.0003$  Bq/kg for IAEA-384 and  $0.019 \pm 0.002$  Bq/kg for IAEA-385),  $^{239}\text{Pu}$  ( $96.13 \pm 7.89$  Bq/kg for IAEA-384 and  $2.13 \pm 0.33$  Bq/kg for IAEA-385),  $^{240}\text{Pu}$  ( $17.60 \pm 3.80$  Bq/kg for IAEA-384 and  $1.09 \pm 0.07$  Bq/kg for IAEA-385) and  $^{241}\text{Am}$  ( $38.22 \pm 1.15$  Bq/kg for IAEA-384 and  $21.35 \pm 2.63$  Bq/kg for IAEA-385) was observed, and all the measured values for the IAEA-384 and IAEA-385 agreed well with their certificated values (Povinec et al., 2007; Pham et al., 2008). Chemical yield of all transuranium elements in samples ranged from 70% to 90%.

### 2.3. The CDE migration model

The vertical migration of Np, Pu and Am with a concentration of  $C$  ( $\text{Bq}/\text{cm}^3$ ) in marine sediments can be characterized by a one-dimension convection-dispersion equation (CDE) (Tsabaris et al., 2015):

$\frac{\partial C}{\partial t} = D \frac{\partial^2 C}{\partial x^2} - v \frac{\partial C}{\partial x} - \lambda C$  (1) where  $D$  ( $\text{cm}^2/\text{y}$ ) is the effective dispersion coefficient;  $v$  ( $\text{cm}/\text{y}$ ) is the effective convection velocity;  $\lambda$  ( $\text{y}^{-1}$ ) is the decay constant;  $t$  ( $\text{y}$ ) is the time since radionuclide deposition to the surface sediment and  $x$  ( $\text{cm}$ ) is the sediment depth. Given the relatively slow migration rate of nuclides, the surrounding environment is usually assumed to be relatively uniform and stable, such as the constant amount of particulate matter and water content (Kirchner et al., 2009). Due to the long half-lives of  $^{237}\text{Np}$ ,  $^{239,240}\text{Pu}$  and  $^{241}\text{Am}$ , their decay can also be ignored in the solution to Equation (1).

Since Np, Pu and Am in sediment samples originate from human nuclear activities which mainly occurred in the early 1960s, the input of radionuclides to the sediment can be treated like a single pulse. The following simplified solution has been widely used (Bu et al., 2014)

$$C(x, t) = C_0 \frac{1}{\sqrt{2\pi Dt}} e^{-\frac{(x-vt)^2}{4Dt}} \quad (2)$$

where  $C_0$  is the amount of Np, Pu and Am at present, which can be calculated by the measured distribution. Based on the vertical distribution of Np, Pu and Am in the sediment core, the effective dispersion coefficient and effective convection velocity can be fitted. The two sediment cores were fitted by using an unweighted nonlinear least-squares fitting procedure in commercial statistical software (Origin,

2022; Origin Lab, USA).

## 3. Results and discussion

### 3.1. Level and distribution of $^{237}\text{Np}$ , $^{239,240}\text{Pu}$ and $^{241}\text{Am}$ in sediment cores

The concentrations of  $^{237}\text{Np}$ ,  $^{239+240}\text{Pu}$  and  $^{241}\text{Am}$  in the two sediment cores (JS-2 and JS-4) are shown in Fig. 2 and Table S2. The  $^{239+240}\text{Pu}$  concentrations ranged from 0.01 to 2.02 Bq/kg in JS-2 and from 0.15 to 0.66 Bq/kg in JS-4, which are comparable to the  $^{239+240}\text{Pu}$  concentrations of 0.04–3.61 Bq/kg in Japan Sea (Zheng and Yamada, 2005) and 0.002–3.079 Bq/kg in East coast of Japan (Bu et al., 2013). Similarly, the measured  $^{241}\text{Am}$  concentrations (0.02–1.11 Bq/kg in JS-2 and 0.01–0.46 Bq/kg in JS-4) in this work fall into the reported range 0.03–2.40 Bq/kg in Japan Sea (Yamada and Oikawa, 2022).  $^{237}\text{Np}$  concentrations ranged from 0.01 to 1.02 mBq/kg in JS-2 and from 0.11 to 0.78 mBq/kg in JS-4, which are slightly higher than those for Np ( $0.04$ – $0.28$  mBq/kg) in sediment samples near Qinshan and Tianwan nuclear power plants (Ni et al., 2020), and basically consistent with those in Xingkai Lake sediments ( $0.02$ – $2.20$  mBq/kg) (Zhang et al., 2022) and Japan soil samples ( $0.02$ – $2.79$  mBq/kg) (Zheng et al., 2022, 2023). From the perspective of  $^{237}\text{Np}$ ,  $^{239+240}\text{Pu}$  ( $^{239}\text{Pu}$  +  $^{240}\text{Pu}$ ) and  $^{241}\text{Am}$  concentrations, no significant environmental contamination was observed in the investigated area.

As shown in Fig. 2a, the  $^{239+240}\text{Pu}$  activities in JS-2 rapidly increased with the increasing of depth and showed a maximum value at 5–6 cm, and then exponentially decreased along depth. The activity of  $^{241}\text{Am}$  and  $^{237}\text{Np}$  showed a similar distribution as that of  $^{239+240}\text{Pu}$  (Fig. 2b and c) in that their maximum activities occurred at the depth of 5–6 cm. The peak of Pu isotopes at JS-2 are similar to the reported values in sediment core collected from Xingkai Lake (Zhang et al., 2022) and the Japan Sea (Lee et al., 1998). The  $^{239+240}\text{Pu}$  activities in JS-4 (Fig. 2d) gradually increased with increasing depth, with maximum values at 24 cm, which was much deeper than JS-2. This indicated that the sedimentation rate is much higher at this site. Similarly, the maximum activities of  $^{241}\text{Am}$  and  $^{237}\text{Np}$  were observed at the depth of 24 cm (Fig. 2e and f). It should be noted that it is difficult to find the depth of background level with measurable artificial radionuclides, since the sampling depth in the sediment core of JS-4 is only 31 cm.

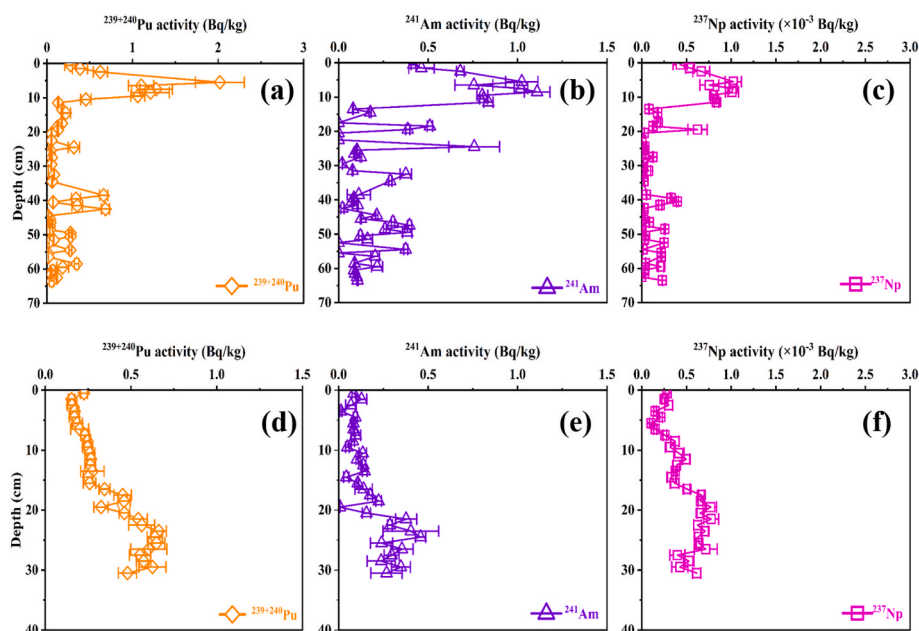


Fig. 2. Vertical distributions of  $^{239+240}\text{Pu}$ ,  $^{241}\text{Am}$  and  $^{237}\text{Np}$  in cores JS-2 (a, b and c) and JS-4 (d, e and f).

### 3.2. Sources of Pu isotopes, $^{237}\text{Np}$ and $^{241}\text{Am}$ in Peter the Great Bay of Japan sea

The inventory and the ratio of radionuclides are generally used for source identification (Zheng and Yamada, 2004). The inventory of  $^{239+240}\text{Pu}$  in JS-2 and JS-4 cores were estimated to be  $87.79\text{ Bq/m}^2$  and  $54.06\text{ Bq/m}^2$  respectively, which was consistent with the reported values ( $66.2\text{--}99.5\text{ Bq/m}^2$ ) (Hong et al., 1999) in Peter the Great Bay. However, the Pu inventory ( $87.79\text{ Bq/m}^2$ ) of JS-2 was higher than that of global fallout ( $58\text{ Bq/m}^2$ ) at  $40\text{--}50^\circ\text{N}$  (Zheng and Yamada, 2005). As shown in Fig. 2, the lower Pu inventory ( $54.06\text{ Bq/m}^2$ ) in JS-4 is attributed to the insufficient sampling depth. Even so, it is reasonable to assume that the Pu inventory in JS-4 could also be higher than that of global fallout. Therefore, apart from the source of global fallout, the  $^{237}\text{Np}$ , Pu isotopes and  $^{241}\text{Am}$  in the study area could originate from the contributions of other nuclear activities.

Based on the specific ratios of  $^{240}\text{Pu}/^{239}\text{Pu}$ ,  $^{241}\text{Am}/^{239+240}\text{Pu}$  and  $^{237}\text{Np}/^{239}\text{Pu}$  of the different sources, these radionuclide ratios could be used for source identification and estimation (Huang et al., 2023a; Wang et al., 2017). Distribution of  $^{240}\text{Pu}/^{239}\text{Pu}$ ,  $^{241}\text{Am}/^{239+240}\text{Pu}$  and  $^{237}\text{Np}/^{239}\text{Pu}$  ratios in the sediment samples of JS-2 and JS-4 is presented in Fig. 3. The results showed that  $^{240}\text{Pu}/^{239}\text{Pu}$  atomic ratios in JS-2 ranged from 0.15 to 0.24 with the average value of  $0.20 \pm 0.02$ , and the ratios in JS-4 ranged from 0.18 to 0.24 with the average value of  $0.21 \pm 0.01$ , which were slightly higher than that of the global fallout of atmospheric nuclear weapon tests at  $30\text{--}71^\circ\text{N}$  ( $0.18 \pm 0.01$ ) (Kelley et al., 1999), suggesting the existence of regional sources in addition to global fallout in the investigated area. It is well known that a large number of nuclear tests were conducted in the PPG in 1946–1962 (Fig. 1) (Liu et al., 2013). The transuranium radionuclides released from underwater tests and close-in fallout in the PPG were deposited in the marine sediment, which was continuously released to the above water body and transported to the northwest Pacific Ocean, such as the China seas and even the Japan Sea, through the ocean currents of the North Equatorial Current and the Kuroshio Current (Zheng and Yamada, 2004; Wu et al., 2014). The  $^{240}\text{Pu}/^{239}\text{Pu}$  atomic ratio of PPG was reported to be 0.30–0.36 (Zheng and Yamada, 2005), which could potentially contribute to the elevated Pu inventory in the northwest of Japan Sea

through the prevailing ocean currents transporting Pu derived from the PPG. It can be seen in Fig. 3b and e that the average values of  $^{241}\text{Am}/^{239+240}\text{Pu}$  activity ratios in JS-2 and JS-4 are  $3.32 \pm 2.76$  and  $0.45 \pm 0.17$ , respectively, which were obviously higher than that of global fallout value ( $0.35$  corrected to 2022) (Zheng et al., 2012) and lower than that of PPG value ( $1.02$  corrected to 2022) (Yamada and Oikawa, 2022). This indicated that PPG should be another source of the Pu and Am besides the global fallout in this area.

The K-431 nuclear submarine accident of the Russian Pacific Fleet in Chazhma Bay (Sarkisov and Vysotskii, 2021) might be another source of transuranics in this area. The K-431 nuclear submarine was equipped with a pressurized water reactor. Leakage from the nuclear reactor may have released transuranium radionuclides, in this case, the  $^{240}\text{Pu}/^{239}\text{Pu}$  atomic ratio is generally greater than 0.4 (Takano et al., 2001; Taylor et al., 2001). The K-431 nuclear submarine accident and Fukushima nuclear accident were reactor accidents. Zheng et al. (2013) has reported that only a trace amount of Pu isotopes ( $\sim 2 \times 10^{-5}\%$  of the core inventory) from the Fukushima accident was released into the environment via atmospheric deposition, and no significant Pu contamination in the near coastal area off Fukushima after the accident was observed. Fukushima accident released about  $150\text{--}160\text{ PBq}$  of  $^{131}\text{I}$  and  $10\text{--}15\text{ PBq}$  of  $^{137}\text{Cs}$  to the atmosphere (Stohl et al., 2012; Hou et al., 2013). Whereas the K-431 nuclear submarine leaked only  $0.35\text{ PBq}$   $^{137}\text{Cs}$  and  $2.9 \times 10^{-5}\text{ PBq}$   $^{131}\text{I}$  to the environment in 1990s (Takano et al., 2001), which were several orders of magnitudes lower than those of Fukushima accident. Therefore, we presume that the contribution of the K-431 accident to the transuranic radionuclides in this sea area is extremely small and can be ignored. In addition, from the perspective of  $^{239+240}\text{Pu}$  and  $^{241}\text{Am}$  activities, no significant contamination of Pu isotopes was observed in this area. Moreover, since no contribution of transuranium radionuclides from the Fukushima accident in neighboring regions at the same latitude (e.g., Japan Sea, Changbai Mountain in northeastern China, Korea Strait) has been observed (Xu et al., 2015; Men et al., 2019; Guan et al., 2023), the contribution of transuranium radionuclides from Chernobyl accident and Fukushima accident in this Bay is likely negligible.

The measured  $^{237}\text{Np}/^{239}\text{Pu}$  atomic ratios in the sediment samples of JS-2 and JS-4 were  $(0.1\text{--}9.2) \times 10^{-4}$  and  $(0.9\text{--}3.5) \times 10^{-4}$ , with a mean

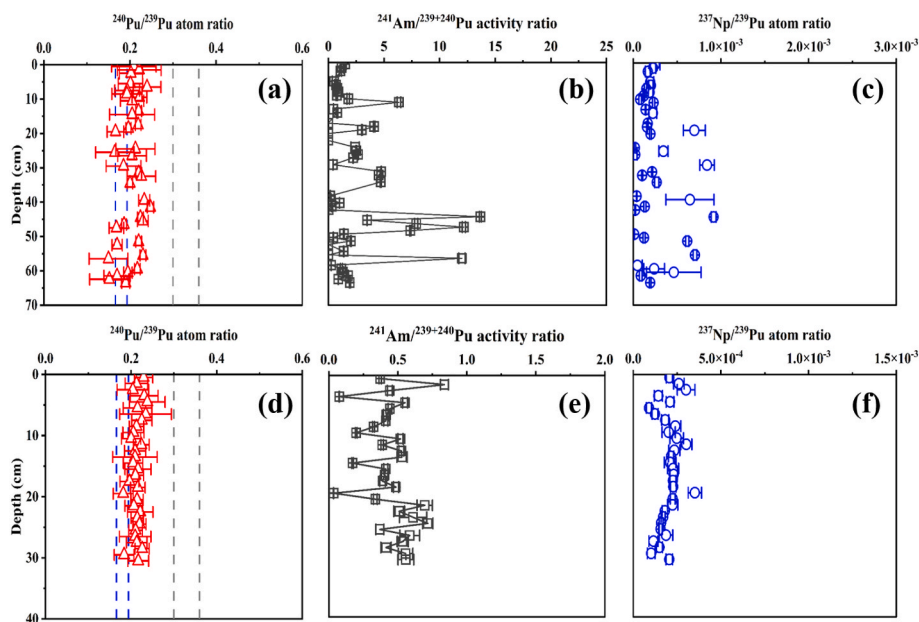


Fig. 3. Distributions of  $^{240}\text{Pu}/^{239}\text{Pu}$  atomic ratio,  $^{241}\text{Am}/^{239+240}\text{Pu}$  activity ratio and  $^{237}\text{Np}/^{239}\text{Pu}$  atomic ratio in cores JS-2 (a, b, c) and JS-4 (d, e, f). Blue dashed lines represent the average  $^{240}\text{Pu}/^{239}\text{Pu}$  atomic ratio ( $0.180 \pm 0.014$ ) of global fallout (Kelley et al., 1999) and gray dashed lines represent the  $^{240}\text{Pu}/^{239}\text{Pu}$  atomic ratio (0.30–0.36) characteristic of the Pacific Proving Ground (PPG) (Buesseler, 1997). (For interpretation of the references to colour in this figure legend, the reader is referred to the Web version of this article.)

value of  $(2.5 \pm 2.4) \times 10^{-4}$  and  $(2.0 \pm 0.5) \times 10^{-4}$ , respectively (Fig. 3c and f), which were obviously lower than the characteristic value of global fallout of atmospheric nuclear weapon tests ( $0.48 \pm 0.07$ ) (Kelley et al., 1999). The low  $^{237}\text{Np}/^{239}\text{Pu}$  atomic ratio in the investigated area might mainly be attributed to the different chemical properties and environmental behaviors of plutonium and neptunium in the marine system. Neptunium commonly presents as the soluble  $\text{NpO}_2^+$  in seawater, and therefore was less prone to sediment deposition (Ni et al., 2020). Therefore, the  $^{237}\text{Np}/^{239}\text{Pu}$  atomic ratio for source identification in sediment samples could be limited in view of their different physical and chemical behaviors in the ocean.

### 3.3. Resolving global fallout and PPG

Two end-members meta-mixing models have been widely used for the estimation of contribution between global fallout and PPG in this field of study (Liu et al., 2011; Wu et al., 2014). To better understand the two-end member meta-mixing model, we plotted in Fig. 4 the relationship between the  $^{240}\text{Pu}/^{239}\text{Pu}$  atomic ratio and the  $^{239+240}\text{Pu}$  activity ( $^{239}\text{Pu} + ^{240}\text{Pu}$ ) for two sediment cores. All data falls between the characteristic values of global fallout and PPG, and the sources of Pu in both sediment cores are dominated by global fallout of atmospheric nuclear weapon tests.

A simple two-end member mixing model (Kelley et al., 1999) was applied to quantitatively estimate the contribution of PPG and global fallout to the Sea of Japan waters by:

$$\frac{(\text{Pu})_P}{(\text{Pu})_G} = \frac{(R_G - R_S)(1 + 3.67R_P)}{(R_S - R_P)(1 + 3.67R_G)}$$

$$(\text{Pu})_P + (\text{Pu})_G = 100\% \quad (4)$$

where (Pu) and R represent the  $^{239+240}\text{Pu}$  activity and the  $^{240}\text{Pu}/^{239}\text{Pu}$  atomic ratio, respectively; the subscripts of P, G and S refer to the PPG, Global fallout and Japan Sea, respectively. The value 3.67 is a factor used to convert between the activity and the atom ratio of  $^{240}\text{Pu}/^{239}\text{Pu}$ .  $R_G$  and  $R_P$  were taken to be  $0.180 \pm 0.014$  and  $0.33 \pm 0.03$  (Zheng and

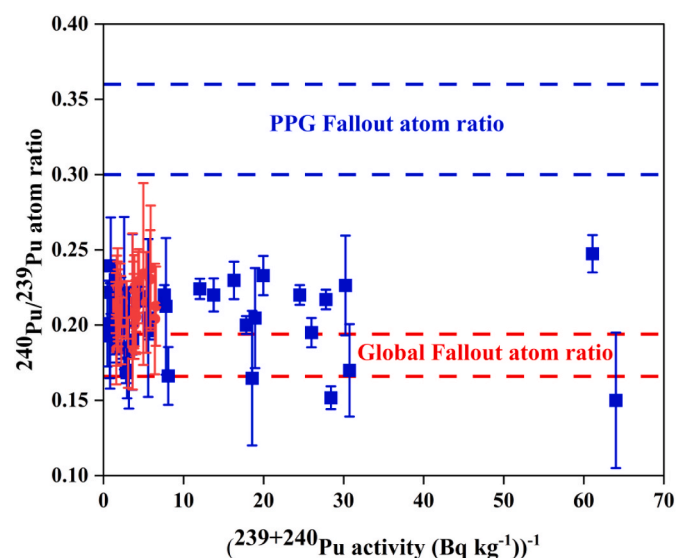


Fig. 4. Relationship between  $^{240}\text{Pu}/^{239}\text{Pu}$  atomic ratio and the reciprocal of  $^{239+240}\text{Pu}$  activity ( $^{239}\text{Pu} + ^{240}\text{Pu}$ ) for sediments in the Japan Sea. The blue squares represent the JS-2 data and the red circles indicate the JS-4 data. Blue dashed lines represent the  $^{240}\text{Pu}/^{239}\text{Pu}$  atomic (0.30–0.36) (Buesseler, 1997) of PPG and red dashed lines indicate the  $^{240}\text{Pu}/^{239}\text{Pu}$  atomic ratio ( $0.180 \pm 0.014$ ) of global fallout (Kelley et al., 1999). (For interpretation of the references to colour in this figure legend, the reader is referred to the Web version of this article.)

Yamada, 2005; Wu et al., 2014). The results showed that the contribution of the PPG close-in fallout to the JS-2 and the JS-4 were in the range of  $18\% \pm 8\%$  and  $27\% \pm 10\%$ , with the average of  $23\% \pm 6\%$  in the investigated area, which was consistent with the reported results (20%–23%) in Japan Sea (Zheng and Yamada, 2005). The results in this work were much lower than the contribution of PPG to the South China Sea (ca. 57%) (Dong et al., 2010), East China Sea (ca. 45%) (Liu et al., 2011), the eastern coast of Japan (ca. 40%) (Bu et al., 2013). The transport pathway of Pu from the PPG to the Japan Sea is shown in Fig. S1. Briefly, it is hypothesized that the water mass carried transuranium radionuclides from PPG to the Northwest Pacific Ocean under the influence of the North Equatorial Current and the Kuroshio Current, and then a branch of the Kuroshio carried transuranium radionuclides to the Japan Sea through the Tsushima Strait.

### 3.4. Migration of Pu isotopes, $^{237}\text{Np}$ and $^{241}\text{Am}$ in Japan sea

The activity peaks of  $^{237}\text{Np}$ , Pu isotopes and  $^{241}\text{Am}$  were located at the layer of 5.5 cm and 24 cm in the sediment cores of JS-2 and JS-4, respectively (Fig. 2). This distribution records the sedimentation history of radionuclides in the investigated area. According to the principle of these radionuclides as a time mark for sediment dating, the position of the maximum peak could be marked as the year of 1964 since the main source of transuranium radionuclides in the investigated ocean was the global fallout of atmospheric nuclear weapon tests peaked in 1962 and 2 years lag between atmospheric weapons tests and the deposition on the sea bed (Aarkrog, 2003; Zheng and Yamada, 2005; Hou and Roos, 2008). The mean sedimentation rate in JS-2 was thus estimated to be 0.09 cm/y, which was generally comparable to the results of Lee et al. (1998) in the southern part of this study area (0.06–0.07 cm/y) (Lee et al., 1998) and the Amur Bay (ca. 0.05 cm/y) (Kuzmenkova et al., 2023). However, a much higher sedimentation rate 0.41 cm/y was estimated at JS-4. The sediment core of JS-4 was collected in the Ussuri Bay (Fig. 1). The rapid development of industrialization in Peter the Great Bay region in recent years has led to the increase of agricultural activities. Several large rivers (Knevichanka River, Artemovka River, Shkotovka River, Lazurnaya River, etc.) flowing to the Ussuri Bay (Semkin et al., 2015) could carry large amount of particulate matter to Ussuri bay and increase the sedimentation rate.

For the investigation of the migration of transuranium radionuclides in the sedimentary environment, the vertical distribution of radionuclides in the sedimentary column was fitted using the CDE model. The fitting curve and experimental results are shown in Fig. S2. The fitting parameters of JS-2 were slightly lower than JS-4 (Table 1). This might be related to the sea current, particle size, pH, organic content and other factors of the two sedimentary columns (Kirchner et al., 2009).

Based on the fitting parameters of the CDE model, the migrations of Np, Pu and Am at different time scales (50, 100, 200 and 500 years) in the sediment core of JS-2 and JS-4 were predicted. The results (Fig. 5) showed that the peak values of Np, Pu and Am activities gradually decreased during migration, and the width of the peak gradually widened. The peak of Np, Pu and Am in JS-2 will migrate to about 75 cm after 500 years, while the peak in JS-4 is about 200 cm after 500 years.

## 4. Conclusions

This study investigated the level, distribution and sources of Np, Pu

Table 1

The obtained parameters  $v$  and  $D$  for  $^{237}\text{Np}$ ,  $^{239+240}\text{Pu}$  and  $^{241}\text{Am}$  in the Japan Sea fitted to the CDE model.

| Sample site | $^{237}\text{Np}$ |      | $^{239+240}\text{Pu}$ |      | $^{241}\text{Am}$ |      |
|-------------|-------------------|------|-----------------------|------|-------------------|------|
|             | $v$               | $D$  | $v$                   | $D$  | $v$               | $D$  |
| JS-2        | 0.14              | 0.3  | 0.13                  | 0.1  | 0.15              | 0.27 |
| JS-4        | 0.47              | 1.63 | 0.71                  | 3.69 | 0.63              | 1.68 |

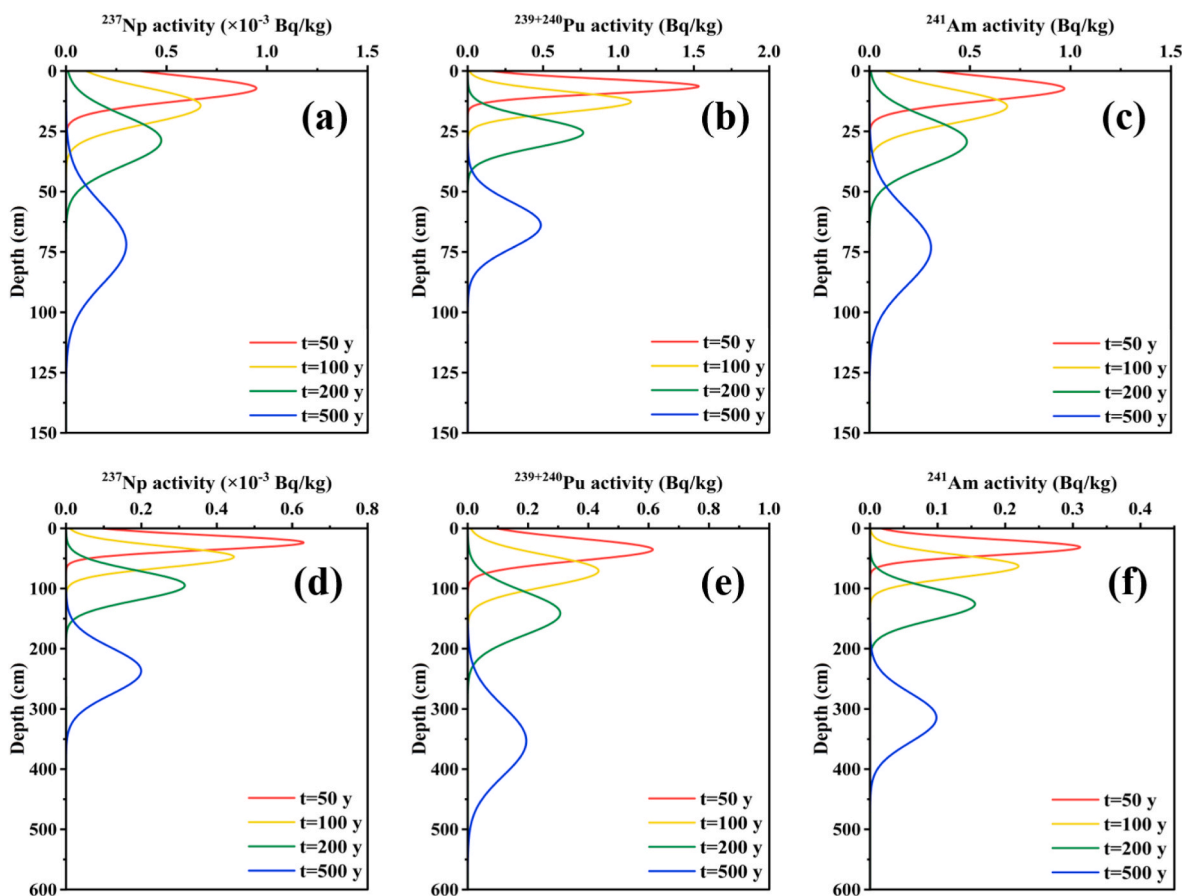


Fig. 5. Illustration of the downward migrations of Pu isotopes,  $^{237}\text{Np}$  and  $^{241}\text{Am}$  in JS-2(a, b, c) and JS-4(d, e, f) predicted by the CDE model after deposition in 1964.

and Am in the Peter the Great Bay of Japan Sea, and revealed the impact of the K-431 nuclear submarine accident on the surrounding environment after more than three decades. Based on the results and discussion above, it can be concluded: (1) The concentrations of  $^{237}\text{Np}$  (0.01–1.02 mBq/kg),  $^{239,240}\text{Pu}$  (0.01–1.11 Bq/kg) and  $^{241}\text{Am}$  (0.01–2.02 Bq/kg) in all sediment samples fell in the range of the reported values in this area. (2) Based on the average of  $^{240}\text{Pu}/^{239}\text{Pu}$  atomic ratios ( $0.20 \pm 0.02$  and  $0.21 \pm 0.01$ ) and  $^{241}\text{Am}/^{239+240}\text{Pu}$  activity ratios ( $3.32 \pm 2.76$  and  $0.45 \pm 0.17$ ) in two sediment cores, the transuranium radionuclides originated from the global fallout and PPG. The contributions of PPG and the global fallout were calculated to be  $23\% \pm 6\%$  and  $77\%$  in this area, respectively. The results indicated that the prevailing ocean currents could carry radionuclides derived from the PPG to the investigated area. (3) There is no measurable release of transuranium radionuclides from the local K-431 submarine nuclear incident, and any contribution to the local marine environment is negligible. (4) From the perspective of  $^{237}\text{Np}$  concentrations and  $^{237}\text{Np}/^{239}\text{Pu}$  atomic ratios,  $^{237}\text{Np}$  is not suitable for source identification.

#### CRedit authorship contribution statement

**Jiang Sun:** Writing – review & editing, Writing – original draft, Investigation, Data curation. **Shaodong Zhu:** Methodology, Data curation. **Shan Xing:** Writing – review & editing, Supervision, Resources, Conceptualization. **Natalia V. Kuzmenkova:** Writing – review & editing, Investigation. **Chenyang Peng:** Methodology, Investigation. **Yiman Lu:** Software, Methodology. **Alexandra Rozhkova:** Investigation, Data curation. **Vladimir G. Petrov:** Investigation. **Keliang Shi:** Writing – review & editing, Supervision. **Stepan N. Kalmykov:** Writing – review & editing, Funding acquisition. **Xiaolin Hou:** Writing – review & editing, Supervision, Project administration, Funding acquisition.

#### Declaration of competing interest

The authors declare that they have no known competing financial interests or personal relationships that could have appeared to influence the work reported in this paper.

#### Data availability

Data will be made available on request.

#### Acknowledgments

The study was supported by the National Nature Science Foundation of China (NSFC) (No. 12175201) and the Russian Science Foundation (RSF) (project No. 21-43-00025), as part of an RSF-NSFC cooperation project as well as National Nature Science Foundation of China (NSFC) (No. 22061132004).

#### Appendix A. Supplementary data

Supplementary data to this article can be found online at <https://doi.org/10.1016/j.jenvrad.2024.107400>.

#### References

- Aarkrog, A., 2003. Input of anthropogenic radionuclides into the world ocean. Deep Sea Res. Part II Top. Stud. Oceanogr. 50 (17–21), 2597–2606. [https://doi.org/10.1016/S0967-0645\(03\)00137-1](https://doi.org/10.1016/S0967-0645(03)00137-1).
- Assinder, D.J., 1999. A review of the occurrence and behaviour of neptunium in the Irish Sea. J. Environ. Radioact. 44 (2–3), 335–347. [https://doi.org/10.1016/S0265-931X\(98\)00139-8](https://doi.org/10.1016/S0265-931X(98)00139-8).
- Beasley, T.M., Kelley, J.M., Orlandini, K.A., et al., 1998. Isotopic Pu, U, and Np signatures in soils from semipalatinsk-21, Kazakh republic and the southern urals,

- Russia. *J. Environ. Radioact.* 39 (2), 215–230. [https://doi.org/10.1016/S0265-931X\(97\)00050-7](https://doi.org/10.1016/S0265-931X(97)00050-7).
- Bu, W.T., Zheng, J., Guo, Q.J., Uchida, S., 2014. Vertical distribution and migration of global fallout Pu in forest soils in southwestern China. *J. Environ. Radioact.* 136, 174–180. <https://doi.org/10.1016/j.jenvrad.2014.06.010>.
- Bu, W.T., Zheng, J., Aono, T., et al., 2013. Vertical distributions of plutonium isotopes in marine sediment cores off the Fukushima coast after the Fukushima Dai-ichi Nuclear Power Plant accident. *Biogeosciences* 10 (4), 2497–2511. <https://doi.org/10.5194/bg-10-2497-2013>.
- Buesseler, K., 1997. The isotopic signature of fallout plutonium in the North Pacific. *J. Environ. Radioact.* 36 (1), 69–83. [https://doi.org/10.1016/S0265-931X\(96\)00071-9](https://doi.org/10.1016/S0265-931X(96)00071-9).
- Buesseler, K., Dai, M.H., Aoyama, M., et al., 2017. Fukushima daiichi-derived radionuclides in the ocean: transport, fate, and impacts, annual review of marine science. *Ann. Rev. Mar. Sci.* 9, 173–203. <https://doi.org/10.1146/annurev-marine-010816-060733>.
- Dai, M.H., Kelley, J.M., Buesseler, K.O., 2002. Sources and migration of plutonium in groundwater at the savannah river site. *Environ. Sci. Technol.* 36 (17), 3690–3699. <https://doi.org/10.1021/es020025t>.
- Dong, W., Zheng, J., Guo, Q.J., et al., 2010. Characterization of plutonium in deep-sea sediments of the sulu and south China seas. *J. Environ. Radioact.* 101 (8), 622–629. <https://doi.org/10.1016/j.jenvrad.2010.03.011>.
- Dozol, M., Hagemann, R., Hoffman, D.C., et al., 1993. Radionuclide migration in groundwaters—Review of the behavior of actinides. *Pure Appl. Chem.* 65 (5), 1081–1102. <https://doi.org/10.1351/pac199365051081>.
- Guan, Y.J., Wang, S.Z., Jing, Q.Y., et al., 2023. Sequential extraction of  $^{239+240}\text{Pu}$  and the vertical distribution of  $^{239+240}\text{Pu}$ ,  $^{137}\text{Cs}$ , and heavy metals in chang-Bai mountains' grassland soil. *ACS Earth Space Chem.* 7 (1), 182–194. <https://doi.org/10.1021/acsearthspacechem.2c00286>.
- Hong, G.H., Kim, S.H., Lee, S.H., et al., 1999. Artificial radionuclides in the East sea (Sea of Japan) proper and peter the Great bay. *Mar. Pollut. Bull.* 38 (10), 933–943. [https://doi.org/10.1016/S0025-326X\(99\)00107-1](https://doi.org/10.1016/S0025-326X(99)00107-1).
- Hou, X.L., Roos, P., 2008. Critical comparison of radiometric and mass spectrometric methods for the determination of radionuclides in environmental, biological and nuclear waste samples. *Anal. Chim. Acta* 608 (2), 105–139. <https://doi.org/10.1016/j.aca.2007.12.012>.
- Hou, X.L., Povinec, P.P., Zhang, L.Y., et al., 2013. Iodine-129 in seawater offshore Fukushima: distribution, inorganic speciation, sources, and budget. *Environ. Sci. Technol.* 47 (7), 3091–3098. <https://doi.org/10.1021/es304460k>.
- Huang, C.P., Guan, Y.J., Wang, D.Y., et al., 2023a. Distribution characteristics of radionuclides ( $^{137}\text{Cs}$ ,  $^{239+240}\text{Pu}$ ,  $^{237}\text{Np}$ , and  $^{241}\text{Am}$ ) in vertical vegetation zone in Changbai Mountain, China. *Catena* 225, 107017. <https://doi.org/10.1016/j.catena.2023.107017>.
- Huang, Z., Hou, X.L., Zhao, X., 2023b. Rapid and simultaneous determination of  $^{238}\text{Pu}$ ,  $^{239}\text{Pu}$ ,  $^{240}\text{Pu}$ , and  $^{241}\text{Pu}$  in samples with high-level uranium using ICP-MS/MS and extraction chromatography. *Anal. Chem.* 95 (35), 12931–12939. <https://doi.org/10.1021/acs.analchem.3c02526>.
- Ikeuchi, Y., 2003. Temporal variations of  $^{90}\text{Sr}$  and  $^{137}\text{Cs}$  concentrations in Japanese coastal surface seawater and sediments from 1974 to 1998. *Deep Sea Res. Part II Top. Stud. Oceanogr.* 50 (17–21), 2713–2726. [https://doi.org/10.1016/S0967-0645\(03\)00143-7](https://doi.org/10.1016/S0967-0645(03)00143-7).
- Kelley, J.M., Bond, A.H., Beasley, T.M., 1999. Global distribution of Pu isotopes and  $^{237}\text{Np}$ . *Sci. Total Environ.* 238, 483–500. [https://doi.org/10.1016/S0048-9697\(99\)00160-6](https://doi.org/10.1016/S0048-9697(99)00160-6).
- Kirchner, G., Strebl, F., Bossew, P., et al., 2009. Vertical migration of radionuclides in undisturbed grassland soils. *J. Environ. Radioact.* 100 (9), 716–720. <https://doi.org/10.1016/j.jenvrad.2008.10.010>.
- Kuzmenkova, N., Rozhkova, A., Egorin, A., et al., 2023. Analysis of sedimentation processes in lake khanka (xingkaihu) and Amur bay using  $^{137}\text{Cs}$  and  $^{210}\text{pb}_{\text{ex}}$  tracers. *J. Radioanal. Nucl. Chem.* 332 (4), 959–971. <https://doi.org/10.1007/s10967-023-08813-8>.
- Lee, M.H., Lee, C.W., Moon, D.S., et al., 1998. Distribution and inventory of fallout Pu and Cs in the sediment of the East Sea of Korea. *J. Environ. Radioact.* 41 (2), 99–110. [https://doi.org/10.1016/S0265-931X\(98\)00011-3](https://doi.org/10.1016/S0265-931X(98)00011-3).
- Liu, Z.Y., Zheng, J., Pan, S.M., et al., 2011. Pu and  $^{137}\text{Cs}$  in the yangtze river estuary sediments: distribution and source identification. *Environ. Sci. Technol.* 45 (5), 1805–1811. <https://doi.org/10.1021/es1035688>.
- Liu, Z.Y., Zheng, J., Pan, S.M., et al., 2013. Anthropogenic plutonium in the North jiangsu tidal flats of the yellow sea in China. *Environ. Monit. Assess.* 185, 6539–6551. <https://doi.org/10.1007/s10661-012-3045-7>.
- Men, W., Zheng, J., Wang, H., et al., 2019. Pu isotopes in the seawater off Fukushima Daiichi Nuclear Power Plant site within two months after the severe nuclear accident. *Environ. Pollut.* 246, 303–310. <https://doi.org/10.1016/j.envpol.2018.12.007>.
- Ni, Y.Y., Guo, Q.J., Huang, Z.Y., et al., 2020. First study of  $^{237}\text{Np}$  in Chinese soils: source, distribution and mobility in comparison with plutonium isotopes. *Chemosphere* 253, 126683. <https://doi.org/10.1016/j.chemosphere.2020.126683>.
- Povinec, P.P., Pham, M.K., Sanchez-Cabeza, J.A., et al., 2007. Reference material for radionuclides in sediment IAEA-384 (Fangataufa Lagoon sediment). *J. Radioanal. Nucl. Chem.* 273 (2), 383–393. <https://doi.org/10.1007/s10967-007-6898-4>.
- Pham, M.K., Sanchez-Cabeza, J.A., Povinec, P.P., et al., 2008. A new Certified Reference Material for radionuclides in Irish sea sediment (IAEA-385). *Appl. Radiat. Isot.* 66 (11), 1711–1717. <https://doi.org/10.1016/j.apradiso.2007.10.020>.
- Sarkisov, A.A., Vysotskii, V.L., 2021. The largest nuclear accident in the history of the nuclear fleet. Reconstruction of events and analysis of the accident consequences to assess the risks and hazards of small nuclear power facilities. *Nucl. Eng. Des.* 384, 111440. <https://doi.org/10.1016/j.nucengdes.2021.111440>.
- Semkin, P.Y., Tishchenko, Y.P., Khodoreenko, N.D., et al., 2015. Production-destruction processes in estuaries of the rivers of Artemovka and Shkotovka (usuri bay) in summer. *Water Resour.* 42 (3), 352–361. <https://doi.org/10.1134/S0097807815030161>.
- Stohl, A., Seibert, P., Wotawa, G., et al., 2012. Xenon-133 and caesium-137 releases into the atmosphere from the Fukushima Dai-ichi nuclear power plant: determination of the source term, atmospheric dispersion, and deposition. *Atmos. Chem. Phys.* 12 (5), 2313–2343. <https://doi.org/10.5194/acp-12-2313-2012>.
- Takano, M., Romanova, V., Yamazawa, H., et al., 2001. Reactivity accident of nuclear submarine near Vladivostok. *J. Nucl. Sci. Technol.* 38 (2), 143–157. <https://doi.org/10.1080/18811248.2001.9715017>.
- Taylor, R.N., Warneke, T., Milton, J.A., et al., 2001. Plutonium isotope ratio analysis at femtogram to nanogram levels by multicollector ICP-MS. *J. Anal. At. Spectrom.* 16 (3), 279–284. <https://doi.org/10.1039/b009078f>.
- Tsabarlis, C., Patiris, D.L., Fillis-Tsirakis, E., et al., 2015. Vertical distribution of  $^{137}\text{Cs}$  activity concentration in marine sediments at Amvrakikos Gulf, western of Greece. *J. Environ. Radioact.* 144, 1–8. <https://doi.org/10.1016/j.jenvrad.2015.02.009>.
- Wang, F.F., Zheng, J., Aono, T., et al., 2022. Source and distribution characteristics of  $^{239}$ ,  $^{240}$ ,  $^{241}\text{Pu}$ ,  $^{237}\text{Np}$  and  $^{134}$ ,  $^{137}\text{Cs}$  in sediments in the Northwest and central equatorial pacific after the Fukushima nuclear accident. *Environ. Pollut.* 304, 119214. <https://doi.org/10.1016/j.envpol.2022.119214>.
- Wang, J.L., Baskaran, M., Hou, X.L., et al., 2017. Historical changes in  $^{239}\text{Pu}$  and  $^{240}\text{Pu}$  sources in sedimentary records in the East China Sea: implications for provenance and transportation. *Earth Planet Sci. Lett.* 466, 32–42. <https://doi.org/10.1016/j.epsl.2017.03.005>.
- Wu, J.W., Zheng, J., Dai, M.H., et al., 2014. Isotopic composition and distribution of plutonium in northern south China sea sediments revealed continuous release and transport of Pu from the Marshall Islands. *Environ. Sci. Technol.* 48 (6), 3136–3144. <https://doi.org/10.1021/es405363q>.
- Xing, S., Zhang, W.C., Qiao, J.X., Hou, X.L., 2018. Determination of ultra-low level plutonium isotopes ( $^{239}\text{Pu}$ ,  $^{240}\text{Pu}$ ) in environmental samples with high uranium. *Talanta* 187, 357–364. <https://doi.org/10.1016/j.talanta.2018.05.051>.
- Xing, S., Peng, C.Y., Christl, M., et al., 2023. Simultaneous determination of transuranium radionuclides for nuclear forensics by compact accelerator mass spectrometry. *Anal. Chem.* 95 (7), 3647–3655. <https://doi.org/10.1021/acs.analchem.2c04544>.
- Xu, Y.H., Qiao, J.X., Pan, S.M., et al., 2015. Plutonium as a tracer for soil erosion assessment in northeast China. *Sci. Total Environ.* 511, 176–185. <https://doi.org/10.1016/j.scitotenv.2014.12.006>.
- Yamada, M., Oikawa, S., 2022.  $^{239}\text{Pu}$ ,  $^{240}\text{Pu}$ ,  $^{241}\text{Pu}$ ,  $^{241}\text{Am}$ ,  $^{137}\text{Cs}$ , and  $^{210}\text{Pb}$  in sea floor sediments in the western North Pacific Ocean and the Sea of Japan: distributions, sources and budgets. *J. Radioanal. Nucl. Chem.* 331 (6), 2689–2703. <https://doi.org/10.1007/s10967-022-08332-y>.
- Yoshida, N., Kanda, J., 2012. Tracking the Fukushima radionuclides. *Science* 336 (6085), 1115–1116. <https://doi.org/10.1126/science.1219493>.
- Zhang, S., Yang, G.S., Zheng, J., et al., 2022. Global fallout Pu isotopes,  $^{137}\text{Cs}$  and  $^{237}\text{Np}$  records in the sediments of Lake Xingkai and their response to environmental changes in the catchment. *Catena* 215, 106276. <https://doi.org/10.1016/j.catena.2022.106276>.
- Zheleznova, A.O., Sun, J., Zhu, S.D., et al., 2024. Sorption behaviour of neptunium in marine and fresh water bottom sediments in Far East area of Russia (Lake Khanka and Amur Bay). *J. Environ. Radioact.* 272, 107334. <https://doi.org/10.1016/j.jenvrad.2023.107334>.
- Zheng, J., Tagami, K., Uchida, S., et al., 2022. Soil-soil solution distribution coefficients of global fallout  $^{239}\text{Pu}$  and  $^{237}\text{Np}$  in Japanese paddy soils. *Chemosphere* 291 (1), 132775. <https://doi.org/10.1016/j.chemosphere.2021.132775>.
- Zheng, J., Tagami, K., Uchida, S., et al., 2023. Assessment of soil-soil solution distribution coefficients of global fallout  $^{237}\text{Np}$  and  $^{239}\text{Pu}$  in Japanese upland soils. *J. Environ. Radioact.* 266, 107241. <https://doi.org/10.1016/j.jenvrad.2023.107241>.
- Zheng, J., Tagami, K., Watanabe, Y., et al., 2012. Isotopic evidence of plutonium release into the environment from the Fukushima DNPP accident. *Sci. Rep.* 2, 304. <https://doi.org/10.1038/srep00304>.
- Zheng, J., Tagami, K., Uchida, S., 2013. Release of plutonium isotopes into the environment from the Fukushima daiichi nuclear power plant accident: what is known and what needs to be known. *Environ. Sci. Technol.* 47 (17), 9584–9595. <https://doi.org/10.1021/es402212v>.
- Zheng, J., Yamada, M., 2004. Sediment core record of global fallout and Bikini close-in fallout Pu in Sagami Bay, western Northwest Pacific margin. *Environ. Sci. Technol.* 38 (13), 3498–3504. <https://doi.org/10.1021/es035193f>.
- Zheng, J., Yamada, M., 2005. Vertical distributions of  $^{239+240}\text{Pu}$  activities and  $^{240}\text{Pu}/^{239}\text{Pu}$  atom ratios in sediment cores: implications for the sources of Pu in the Japan Sea. *Sci. Total Environ.* 340 (1–3), 199–211. <https://doi.org/10.1016/j.scitotenv.2004.09.015>.